2020 17th International Conference on Electrical Engineering, Computing Science and Automatic Control (CCE)
Mexico City, Mexico November 11-13, 2020

A Method to Model the Volume Charge Density in a Multiple-Input Floating-Gate MOS Transistor

Francisco Plascencia Jauregui
Centro Universitario de Ciencias Exactas e Ingenierias
Universidad de Guadalajara
Guadalajara, Mexico
https://orcid.org/0000-0003-4650-6237

Santiago Medina Vazquez
Centro Universitario de Ciencias Exactas e Ingenierias
Universidad de Guadalajara
Guadalajara, Mexico
https://orcid.org/0000-0002-3562-2921

Edwin Becerra Alvarez
Centro Universitario de Ciencias Exactas e Ingenierias
Universidad de Guadalajara
Guadalajara, Mexico
edwincbecerra@gmail.com

Jose Arce Zavala
Centro Universitario de Ciencias Exactas e Ingenierias
Universidad de Guadalajara
Guadalajara, Mexico
https://orcid.org/0000-0003-1533-0494

Sandra Flores Ruiz
Programa Universitario de Lenguas Extranjeras
Universidad de Guadalajara
Guadalajara, Mexico
sandra.flores@proulex.profesor.udg.mx

***Abstract*—We present a methodology to model the volume charge density in the substrate of the Multiple-input Floating-Gate MOS (MIFGMOS) transistor. This method considers the MIFGMOS as an analog CMOS device. We based our procedure on Maxwell's Equations through a Poisson Equation implementation on Matlab. The charges generated during the MIFGMOS polarization, which is made by applying voltages on the Control Gates (CG), are used to calculate electric fields, electric potentials, and finally, the volume charge density in the MIFGMOS transistor channel. Moreover, we introduce a method based on coordinates to generate a mathematical function to describe the electric-potential behavior on the substrate. Finally, we show the volume charge density behavior on three graphics, which allows us to predict regions in which will be a great amount of volume charge density, depending on the voltages of the terminals. The former reveals the relationship between control gates and volume charge density and will allow us to understand and analyze some superior order phenomena.**

***Index Terms*—MIFGMOS, Electric Field, Volume Charge Density, Poisson's Equation**

I. Introduction

The multiple input floating gate transistor [1] is an interesting device because is a proposed option to produce low-voltage and low-power circuits [2]–[4] which are useful in the industry of alternative energy sources [5]. On the other hand, MIFGMOS transistors are able to preform complex operations when they are used in Complementary MOS (CMOS) circuits [6], [7].

MIFGMOS transistor is built by a modification of conventional MOSFET, that means, the isolation of the gate terminal. Then, the polarization is performed applying voltages on Control Gates (CG), as seen in Fig. 1.

Unfortunately, a charge is stored on the floating gate [8] during the MIFGMOS transistor fabrication process. This additional charge modifies the device behavior. This unwanted charge is usually ignored in analysis circuits, for simplicity, but it could be a problem in designing very low voltage circuits. The method proposed in this work, consider the effect of this charge in the volume charge density on the substrate. On the other hand, the method introduced in this paper allow us develop precise and complex models as well as the development of tools that allow simulating circuits that include MIFGMOS.

In addition, although we use Matlab as the developing tool, the device description presented here can be used as assistance for simulating the model of the MIFGMOS transistor in a 3D drift-diffusion code, e.g. Atlas [9].

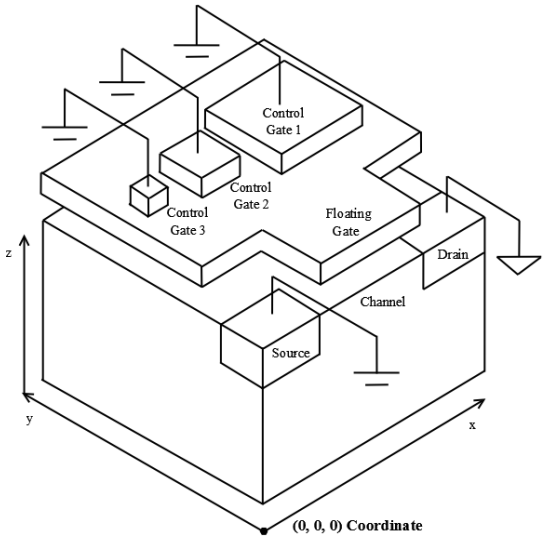

Fig. 1. Isometric projection of a MIFGMOS transistor with three control gates.

We are interested in the use of this device in the analog design environment. Therefore, the main emphasis of this work is on the volume charge density behavior which is formed in the substrate due the effect of the applied voltages on the

control gates. This volume charge density depends on location and dimensions of each control gate.

It is worth mention that this work is about of the volume charge density and the potentials on the substrate. Data obtained could be used in MOSFET models, e.g. EKV and Charge Sheet Model, since we would know the bulk potential and the volume charge density, which would later define the current, and it is proposed as future work. We consider this method as a robust method since it is based on Maxwell Equations.

II. Methods

A. Method Description

The control gates CG_1, CG_2, ..., CG_n, which are made with polisilicon layers, are the electrodes that receive polarization voltage. Theoretically, they have the following characteristics:

- CGs could be range from one to n control gates.
- CGs could have different sizes.
- CGs could have different locations.

In addition, the transistor that we will use will be described according to the Cartesian coordinate system.

MIFGMOS transistor polarization is accomplished by applying voltages on control gates and then generating a difference potential between the drain and the source electrodes. The first step generates a capacitive effect [7] with the polysilicon layer that acts as a floating gate. According to the Polysilicon Depletion Effect [10]–[12] and the Grain Boundary Theory [13], [14], when applying a positive potential, the capacitances create a positive charge density on the floating gate.

This charge density will be take into account as a punctual charge for practical purposes, and it will be located on the inferior face of the polysilicon layer of the floating gate, under the center of each control gate.

Stated in another way, $C_n = Q_n/\Delta V_n$ is the control gate capacitances located between the n plates. Here Q_n is the charge which generated by each control gate and ΔV_n is the voltage generated by each control gate. On the other hand V_{init} is the initial potential that is in the floating gate due to a residual charge formed during the manufacturing process, when the floating gate is isolated. Finally, $V_1, V_2, ..., V_n$, are the applied voltage on the control gates, in such a way that $\Delta V_n = V_n - V_{init}$.

In this document, we will assume as a first approximation, that there is not an initial stored charge in the floating gate, that means $V_{init} = 0$. Therefore, the only potentials to consider are those that are applied to the control gates V_n, then the charge generated by each potential in the floating gate is:

$$Q_n = C_n V_n - C_n V_{init} \tag{1}$$

On the other hand, in order to analyze the channel in several points it is split up into a mesh. In this way, each region has a different distance with respect to every punctual charge Q_n, $n = 1, 2, ..., n$, generated by each control gate. The distance between every punctual charge and each region is measured from the origin of the punctual charge, with coordinates r, to the vertex on the mesh with coordinates r_n, generating the vector $|r - r_n|$, with direction to the unitary vector a_n.

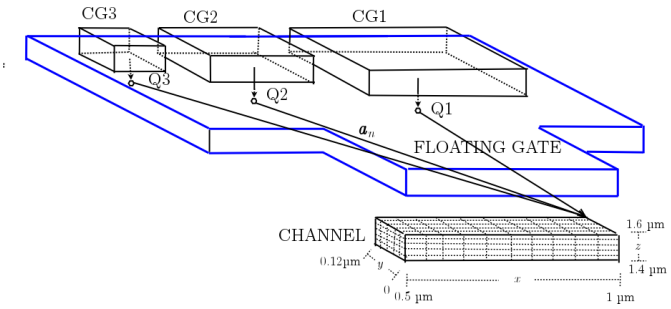

Fig. 2. Calculation of the CGP on a channel point.

Now, we calculate the total potential on each region of the channel due to the action of each punctual charge on the floating gate, which were obtained with (1), using the following relation:

$$V = \sum_{n=1} \frac{Q_n}{4\pi\varepsilon_0 |r - r_n|} \tag{2}$$

where Q_n indicates the value of the involved charges for the obtention of the electric field, and $n = \{1, 2, ..., n\}$.

According to (2), each punctual charge generates a potential in a specific point inside every channel region, and this potential is proportional to the punctual charge magnitude and inversely proportional to $|r - r_n|$.

After obtaining the potential on each region of the meshed channel, these are added to obtain the total potential. If we take all the obtained values in a specific depth plane, it is possible to propose a mathematical function to describe the potential behavior for this layer.

1) Control Gate Potential and Drain-to-Source Potential: We will name *Control-Gate Potential (CGP)* to the potential generated in the channel due to punctual charges on the floating gate, and which is obtained with (2).

Then, a polynomial function is proposed to describe the CGP behavior. This potential will be analyzed by planes on the z-axis, that is, to different depths in the channel. In order to obtain a different plane in different depth, we need a third-grade function of x, y and z coordinates. We propose that the z value will be constant for all the points in each layer of the channel. The function for the CGP must be of third order in z, because it will subsequently be derived twice, this to obtain the final volume density charge.

Due to the z value is fixed and is equal to the depth of the plane, the rest of the CGP will be described in terms of x and y. Then, to have an optimum level of precision, we will use the Curve Fitting tool of Matlab to obtain a third-grade polynomial with all the data obtained with (2) over the plane in z of the mesh, this to obtain the function to describe the potential behavior in the substrate, without still consider the physical parameters of the substrate.

Then, taking into consideration the former, we will have a polynomial function that describes the CGP behavior on the top layer of the channel, and this will have the following form:

$$\begin{aligned} CGP = {} & A \cdot z^3 + B + C \cdot x + D \cdot y + E \cdot x^2 \\ & + F \cdot x \cdot y + G \cdot y^2 + H \cdot x^3 + I \cdot x^2 \cdot y \\ & + J \cdot x \cdot y^2 + K \cdot y^3 \end{aligned} \tag{3}$$

where A, B,...,K, represent coefficients, whereas z indicates the layer into the channel. In addition, x and y, describe the behavior of the potential in those axes.

As we can see, the first term is a function of z, because it will point to the depth of the channel where the potential is analyzed whereas the rest of the polynomial has the form of a third-grade polynomial in terms of x and y.

The next step is to obtain the electric field that is generated from the CGP (EFCGP), using the gradient of the function that describes this potential, this is:

$$\mathbf{E} = -\nabla V = -\left(\frac{\partial V}{\partial x}\mathbf{a}_x + \frac{\partial V}{\partial y}\mathbf{a}_y + \frac{\partial V}{\partial z}\mathbf{a}_z\right) \tag{4}$$

At this point, we perform the first partial derivative over the polynomial function (3).

On the other hand, based on the second action to polarize the MIFGMOS, when the drain is polarized with some voltage, and the source is grounded, this potential crosses the region of the channel. Besides, we will assume that it uniformly degrades as it gets closer to the source. This potential will be named as the *Drain to Source Potential (DSP)*. In contrast to the CGP, in this case (2) is not used to calculate the DSP potential, but the potential applied to the drain is disseminated along the channel. In this manner, the adjacent zone to drain receives more potential, instead of the region which is next to the source. Next, as in the case of the CGP, we propose a polynomial function to describe the DSP behavior which has the form of (3).

This polynomial function will also be partially derived as CGP using (4). In this way, we found the electric field generated from the DSP (EFDSP).

2) Electric Flux Density and Volume Charge Density: Once we obtained the two EFCGP and EFDSP, we proceed to add each pair of results to obtain the resultant electric field , it is said, the partial derivative for x of CGP will be added to the partial derivative for x of the DSP, and so on. Now we have three expressions forming the resultant electric field, giving us its direction and magnitude. They are shown in Table I, where A, B,...,F are coefficients, and x, y, z are the coordinates.

TABLE I
FORMATION OF RESULTANT ELECTRIC FIELD (REF)

	∂x	∂y	∂z
CGP	Ax+By+Cxy+Dx^2+Ey^2+F	Ax+By+Cxy+Dx^2+Ey^2+F	Az^2
DSP	Ax+By+Cxy+Dx^2+Ey^2+F	Ax+By+Cxy+Dx^2+Ey^2+F	Az^2
REF	Ax+By+Cxy+Dx^2+Ey^2+F	Ax+By+Cxy+Dx^2+Ey^2+F	Az^2

Then, each expression of the resultant electric field is multiplied by the permittivity of silicon to obtain the vector field of the Electric Flux Density, given that:

$$\mathbf{D} = \varepsilon \mathbf{E} \tag{5}$$

where $\varepsilon = \varepsilon_0 \cdot \varepsilon_{Si}$. On the one hand, ε_0 indicates the permittivity of the medium in vacuum.

Now, applying the punctual form of Gauss' Law, in which the divergence of the Electric Flux Density is performed, we obtain the Volume Charge Density, that is:

$$\rho_v = \nabla \cdot \mathbf{D} = \left(\frac{\partial \mathbf{D}_x}{\partial x} + \frac{\partial \mathbf{D}_y}{\partial x} + \frac{\partial \mathbf{D}_z}{\partial z}\right) \tag{6}$$

Finally, based on Poisson's Equation [15], [16], in which the Volume Charge Density can be found and cleared, we can establish a relationship between the procedure explained above and Poisson's Equation, that is:

$$\begin{aligned} \nabla \cdot \nabla V &= -\frac{\rho_v}{\varepsilon} \\ -\nabla \cdot (\varepsilon \nabla V) &= \rho_v \end{aligned} \tag{7}$$

III. RESULTS

A. Numerical Example

We present an example to expose the method.

As mentioned in section II, the Cartesian coordinate system is used to describe the material deposition that forms the analyzed device. All measurements are in micrometers. For this particular example, the first material is Si, which will be deposited from coordinates (0, 0, 0) to (1.5, 1.2, 1.6), and this will be the substrate. The origin of the Coordinate system is shown on Fig. 1.

Then, two portions that will be the source and the drain are doped, according to these coordinates:

- Source: from 0 to 0.5 on x, from 0 to 0.12 on y, and from 1.4 to 1.6 on z.
- Drain: from 1 to 1.5 on x, from 0 to 0.12 on y, and from 1.4 to 1.6 on z.

We can suppose that doping is made with Arsenic at $1{\times}10^{20} cm^{-3}$ density , and Boron at $1{\times}10^{17} cm^{-3}$. Both are made with Gauss distribution [9].

Subsequently, a SiO_2 layer is deposed. The first part ranges from 0 to 1.5 on x and 0 to 0.35 on y, with 0.01 of thickness on z. The second part ranges from 0.35 to 1.2 on y and 1.3 to 1.75 on z.

Later, the polysilicon plate for the floating gate is located in two portions. The first one ranges from 0.5 to 1 on x, from 0 to 0.35 on y, and it has a thickness of 0.1 from 1.61 to 1.71 on z. Whereas the second extends from 0.35 to 1.2 on y and from 0 to 1.5 on x.

The next step is to incorporate an isolator as Si_3N_4 on the following locations: the first place is from 0.5 to 1 on x, from 0 to 0.35 on y, and 1.61 to 1.7 on z. The next is from 0 to 1.5 on x, 0.35 to 1.2 on y, and 1.7 to 5.9 on z.

Finally, the Control Gates are located in the following positions, and they are built with polysilicon deposition:

- Control Gate 1: from 0.85 to 1.45 on *x*, from 0.45 to 1.15 on *y*, from 5.72 to 5.93 on *z*.
- Control Gate 2: from 0.35 to 0.75 on *x*, from 0.6 to 1 on *y*, from 5.72 to 5.93 on *z*.
- Control Gate 3: from 0.05 to 0.25 on *x*, from 0.7 to 0.9 on *y*, from 5.72 to 5.93 on *z*.

The dimensions of the control gate 1 are 0.6 in *x* and 0.7 on *y*; then, its surface is 0.42 μm^2. Regarding the control gate 2, its measurements are 0.4 on *x* and 0.4 on *y*; hence its area is 0.16 μm^2. Finally, the control gate 3 measures 0.2 on *x* and 0.2 on *y*, thus the surface is 0.04 μm^2.

It is worth mentioning that the coordinates of the center of each control gates are listed in table II:

TABLE II
CENTER COORDINATES OF EACH CONTROL GATE.

	x	y	z
CG1	1.15 μm	0.8 μm	1.6 μm
CG2	0.55 μm	0.8 μm	1.6 μm
CG3	0.15 μm	0.8 μm	1.6 μm

As we can see in Fig.1, for simplicity purposes, this device has three different Control Gates sizes, but it can be more.

B. Method Results

The first step of the procedure was to find the charges generated on the floating gate by the voltage applied to the control gates. Each control gate was polarized with 0.5 V, that is, $V_1 = V_2 = V_3 = 0.5V$. With the purpose to use (1), it was taken into consideration the surface of each control gate and the separation between the polysilicon plates mentioned in section II. As a result, we obtained the control gate capacitance values and the charges shown in Table III.

TABLE III
CAPACITANCES AND CHARGES FOR CONTROL GATES.

	Capacitance	**Charge**
CG1	9.2967 E-18 F	4.6483 E-18 C
CG2	3.5416 E-18 F	1.7708 E-18 C
CG3	8.8539 E-19 F	4.4270 E-19 C

As mentioned before, these charges were taken as punctual charges located on coordinates listed in Table II.

Then, these charges generated an electric field that crossed the surface of the channel. The CGP was calculated with (2). With the purpose to obtain it, the following considerations were taken into account:

- On x-axis: 11 points were calculated, from coordinate 0.5 to 1.
- On y-axis: 6 points were calculated, from coordinate 0 to 0.12.
- On z-axis: Since the procedure was initially performed over a plane, z value is a constant; for the surface of the channel, this value is 1.6 μm. To obtain a 3D model, this operation is repeated by changing to a new z plane.

After, as an example of application, a polynomial function to describe the CGP was proposed. For this specific case, the top channel face is located on the coordinate 1.6×10^{-6} in z, which elevated to the third power is 4.1×10^{-18}.

Subsequently, it was intended that the z term in the polynomial function represented the first three decimals of the potential channel value because they are the most significant. For example, the potential located on coordinates (*x*, *y*)=(0.5,0) is 0.014607286 V. Therefore, a value that represents 0.014 was proposed. The coefficient found is 3.418×10^{15}, because when it is multiplied by the value on the z coordinate and raised to their power, we obtain the desired value. As a result, the complete term is $3.418\times10^{15}z^3$.

This 0.014 is subtracted of the CGP, and the Curve Fitting tool of Matlab was employed to find the rest of the polynomial function coefficients in terms of x and y. The complete polynomial function is as follows:

$$\begin{aligned} CGP = {} & 3.4180\times10^{15}z^3 + 0.0003355 + 734.7x \\ & + 620.4y - 3.758\times10^{8}x^2 + 9.597\times10^{7}xy \\ & - 3.614\times10^{8}y^2 - 1.261\times10^{13}x^3 \\ & - 5.049\times10^{13}x^2y - 1.092\times10^{13}xy^2 \\ & - 4.89\times10^{13}y^3 \end{aligned} \tag{8}$$

The next step was to calculate the EFCGP, from the gradient of the function that models the potential behavior and which was proposed before, using (4).

Moreover, the DSP was obtained by polarizing the source and drain electrodes. In this exercise, the source is grounded, whereas the drain was polarized with 1 V. Subsequently, based on the assumption that the voltage degrades uniformly, the same process was followed to propose the function that can describe this behavior. This polynomial is as follows:

$$\begin{aligned} DSP = {} & 1.9531\times10^{16}z^3 - 0.827 + 1.66\times10^{6}x \\ & + 5.81\times10^{-}8y - 0.03544x^2 - 0.1199xy \\ & - 0.1986y^2 + 1.355\times10^{4}x^3 + 5.663\times10^{4}x^2y \\ & + 2.256\times10^{5}xy^2 - 1.504\times10^{5}y^3 \end{aligned} \tag{9}$$

This potential generates its own electric field, in the same way that CGP, the EFDSP was calculated with (4).

A resultant electric field is obtained with both electric fields (EFCGP and EFDSP), to know the real effect over charge carriers in the MIFGMOS transistor channel. It is accomplished by adding the expressions shown in Table I, which were obtained after the partial derivatives from (4).

The next step was to obtain the electric flux density based on the resultant electric field through (5). Finally, the volume charge density in the channel was calculated with (6), which is shown in Fig. 3.

This exercise was performed at different substrate depths (z values) to know the complete behavior of the volume charge

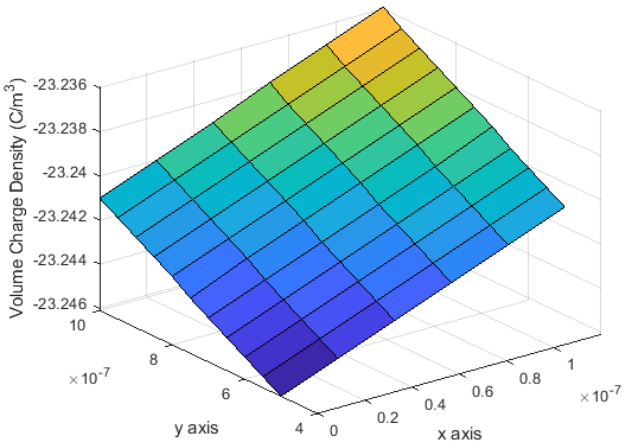

Fig. 3. Volume charge density on substrate surface.

density. It is worth mention that there is a higher concentration of electrons on the substrate surface. The agglutination occurs both longitudinally and transversely. In other words, not only do the electrons gather from left to right (from the source to the drain) but also from front to the back, as we see in Fig. 3. Allowing us to know the behavior of the charge carriers concerning the different electric fields in the MIFGMOS transistor. Moreover, if the transistor entered to the saturation region of operation, a pinch-off would happen in the same direction. The pinch-off phenomenon is the effect whereby the channel depth decreases due to the action of the potential applied to the drain [17]. The former will have implications in a more advanced model and will have to be taken into account in some designs that consider the MIFGMOS as a device for analog circuits.

IV. Discussion

We exposed in the last sections the methodology to obtain the volume charge density in a MIFGMOS transistor substrate. The main discovery of this research is that this volume charge density concentrates not only longitudinally but also transversely over the closer corner to CG1, which is the biggest control gate in this exercise. In other words, the location of the greatest control gate can influence the position and behavior on the substrate of the volume charge density. This relation has not been documented yet. Furthermore, this finding is relevant when a model for the MIFGMOS is developed.

Moreover, we would like to emphasize the fact that at the time the MIFGMOS transistor enters the saturation region of operation, the pinch-off in the channel tends to follow the volume charge density behavior. The former is relevant because of the existence of models based on pinch-of parameter, like the EKV model [18]. As an example of this method, from the volume charge density and without consider some other physical features of the device, we calculated the current on the substrate for different cases of polarization, it is said, to obtain the swept of CG1, both electrodes CG2 and CG3 were fixed to a 0.5 V supply. We used the same procedure for the swept of CG2 and CG3 . This is shown in Fig. 4.

Note that this current is only a representation of the movement of the charge by the effect of the voltage on the control gates, but for a complete model should be taken into account all the physical and electrical parameters inherent to the MOSFET transistor.

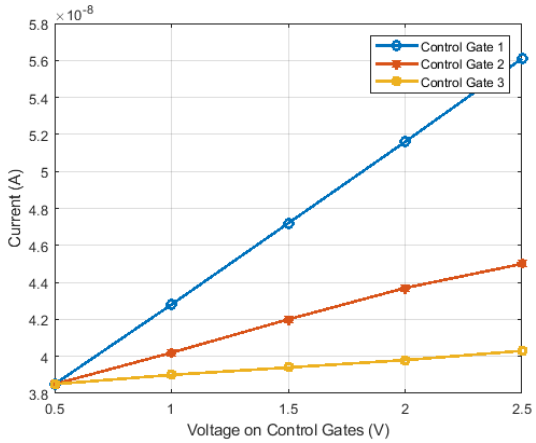

Fig. 4. Current in the substrate generated by the floating gate potential. Swept of CG1 was achieved by fixing both electrodes CG2 and CG3 to a 0.5 V supply. The same procedure was used for sweeping CG2 and CG3.

After, the procedure would permit to consider the cases when there is a residual charge stored in the floating gate due to the fabrication process. On Fig. 5 we appreciate that the volume charge density decreases unlike in Fig.3, when there is a positive residual charge generating 0.1V on the floating gate. On the other hand, Fig. 6 shows an increased volume charge density originated by a negative stored charge generating -0.1V on the floating gate.

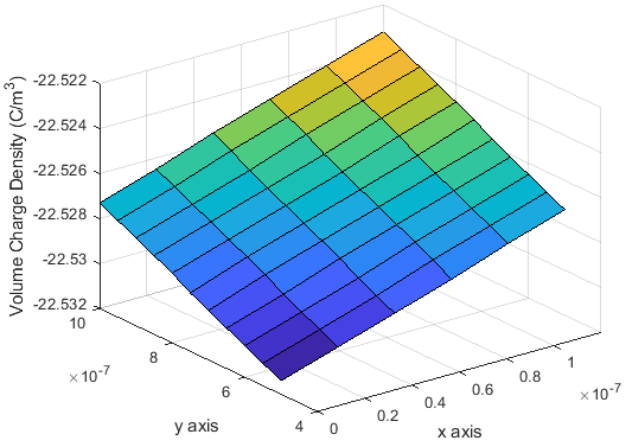

Fig. 5. Volume charge density on substrate surface when there is a positive residual charge on the floating gate.

It is important to mention that the presented method has two limitations. The first one is to consider as punctual

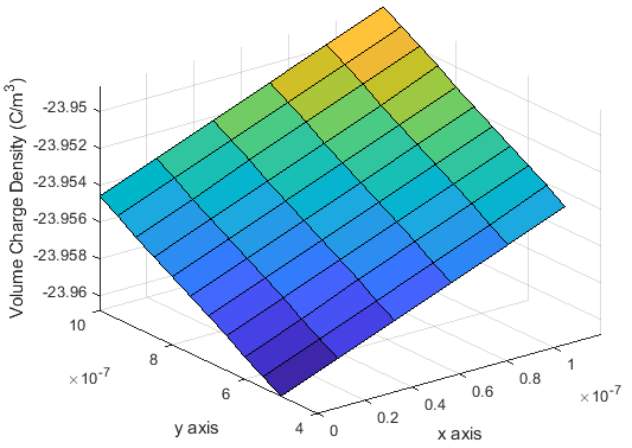

Fig. 6. Volume charge density on substrate surface when there is a negative residual charge on the floating gate.

charges those generated by the polarization of the control gates. Greater precision is would related to evaluating them as surface charges distributed on the polysilicon of the floating gate, and the use of the relation $Q = \int_S \rho_S dS$ which considerably increases the compute requirements.

The second limitation is to consider the uniform degradation of the potential that crosses the channel region from the drain to the source.

This method is the starting point to model other parameters of the device in which we will consider physical parameters as it will be presented in other documents.

Even though these results have not been experimentally proved yet, we started modeling the charge and the potential in the floating gate of the device by using the reliable Maxwell's equations. In addition, the state of the art evidence seems to validate the results we have achieved so far.

Finally, we still have to collect experimental data, but since we are based on Poisson's Equation, the results are qualitatively reliable.

V. Conclusions

A methodology to model the volume charge density in a MIFGMOS transistor substrate was introduced in this article. This method is based on Maxwell's Equations through an implementation on Matlab of the Poisson Equation.

This methodology reveals the relationship between the control gates features as position and dimensions, with the volume charge density behavior. Furthermore, it not only permits to anticipate the behavior of the pinch-off effect but also facilitates to consider and predict the trapped charge in the floating gate due to the fabrication process.

Finally, this method will facilitate the improvement of the MIFGMOS model.

References

[1] T. Shibata, T. Ohmi, "A functional MOS transistor featuring gate-level weighted sum and treshold operations," IEEE Transactions on electron devices, vol. 39, no. 6, pp. 1444-1445, 1992. http://doi.org/10.1109/16.137325

[2] P. Hasler, "Countinous-time feedback in floating-gate MOS circuit," IEEE Systems II: analog and digital signal processing, vol. 48, no. 1, pp. 56-64, 2001. http://doi.org/10.1109/82.913187

[3] A. Basu, "Low-Power, Adaptive Neuromorphic Systems: Recent Progress and Future Directions," IEEE Journal on Emerging and Selected Topics in Circuits and Systems, vol. 8, no. 1, pp. 6-27, 2018. http://doi.org/10.1109/JETCAS.2018.2816339

[4] S. Agarwal, "Using Floating-Gate Memory to Train Ideal Accuracy Neural Networks," IEEE Journal on Exploratory Solid-State Computational Devices and Circuits, vol. 5, no. 1, pp. 52-57, 2019. http://doi.org/10.1109/JXCDC.2019.2902409

[5] E. Sanchez-Sinencio, A.G. Andreou, "Low-Voltage/Low-Power Integrated Circuits and Systems: Low-Voltage Mixed-Signal Circuits," Wiley-IEEE Press, 1999.

[6] E. Rodriguez-Villegas, "Low power and low-voltage circuit design with the FGMOS transistor," Institution of Engineering and Technology, 2006.

[7] A. S. Medina-Vazquez, M. E. Meda-Campana, M. A. Gurrola-Navarro, E. C. Becerra-Alvarez, E. Lopez-Delgadillo, "Analysis of the floating-gate transistor using the charge sheet model," Int. J. Numer. Model., no. 29, pp.675-685, 2016. https://doi.org/10.1002/jnm.2123

[8] E. Rodriguez-Villegas, H. Barnes, "Solution to trapped charge in FGMOS transistors," Electronics letters, vol. 39, no. 19, pp. 1416-1417, 2003. http://doi.org/10.1049/el:20030900

[9] Silvaco, Inc., "Atlas User's Manual : device Simulation Software,", 2015.

[10] R. Rios, N. D. Arora, C. Huang, "An Analytic Polysilicon Depletion Effect Model for MOSFET's," IEEE Electron Device Letters, vol.15, no. 4, pp. 129-131, 1994. http://doi.org/10.1109/55.285407

[11] N. D. Arora, E. Rios, C. Huang, "Modeling the Polysilicon Depletion Effect and Its Impact on Submicrometer CMOS Circuit Performance," IEEE Transactions on Electron Devices, vol.42, no. 5, pp. 935-943, 1995. http://doi.org/10.1109/16.381991

[12] University of California, "BSIM4 4.8.1 MOSFET Model: User's Manual,", 2017.

[13] J. Y. W. Seto, "The electrical properties of polycrystalline silicon films," Journal of Applied Physics, vol. 46, no. 12, pp.5247-5254, 1975. https://doi.org/10.1063/1.321593

[14] T. Nishikawa, K. Ohdaira, H. Matsumura, "Electrical properties of polycrystalline silicon films formed from amorphous silicon films by flash lamp annealing," Current Applied Physics, vol. 11, no. 3, pp. 604-607, 2011. https://doi.org/10.1016/j.cap.2010.10.008

[15] R. Plonsey, R. E. Collin, "Principles and Applications of Electromagnetic Fields," McGraw-Hill, 1961.

[16] W. H. Hayt, J. A. Buck, "Engineering electromagnetics," McGraw-Hill, 2012.

[17] Y. P. Tsividis, C. McAndrew, "Operation and modeling of the MOS transistor," McGraw-Hill, 1987.

[18] C. C. Enz, F. Krummenacher, E. A. Vittoz, "An analytical MOS transistor model valid in all regions of operation and dedicated," Analog Integrated Circuits and Signal Processing, vol. 8, no. 1, 1995. https://doi.org/10.1007/BF01239381